Principal components analysis of Laplacian waveforms as a generic method for identifying ERP generator patterns: II. Adequacy of low-density estimates

Jürgen Kayser [a,b,*], Craig E. Tenke [a,b]

[a] *Department of Biopsychology, New York State Psychiatric Institute, New York, NY, USA*
[b] *Department of Psychiatry, College of Physicians and Surgeons of Columbia University, New York, NY, USA*

Abstract

Objective: To evaluate the comparability of high- and low-density surface Laplacian estimates for determining ERP generator patterns of group data derived from a typical ERP sample size and paradigm.

Methods: High-density ERP data (129 sites) recorded from 17 adults during tonal and phonetic oddball tasks were converted to a 10–20-system EEG montage (31 sites) using spherical spline interpolations. Current source density (CSD) waveforms were computed from the high- and low-density, but otherwise identical, ERPs, and correlated at corresponding locations. CSD data were submitted to separate covariance-based, unrestricted temporal PCAs (Varimax of covariance loadings) to identify and effectively summarize temporally and spatially overlapping CSD components. Solutions were compared by correlating factor loadings and scores, and by plotting ANOVA F statistics derived from corresponding high- and low-resolution factor scores using representative sites.

Results: High- and low-density CSD waveforms, PCA solutions, and F statistics were remarkably similar, yielding correlations of $.9 \leq r \leq .999$ between waveforms, loadings, and scores for almost all comparisons at low-density locations except for low-signal CSD waveforms at occipital sites. Each of the first 10 high-density factors corresponded precisely to one factor of the first 10 low-density factors, with each 10-factor set accounting for the meaningful CSD variance ($>91.6\%$).

Conclusions: Low-density surface Laplacian estimates were shown to be accurate approximations of high-density CSDs at these locations, which adequately and quite sufficiently summarized group data. Moreover, reasonable approximations of many high-density scalp locations were obtained for group data from interpolations of low-density data. If group findings are the primary objective, as typical for cognitive ERP research, low-resolution CSD topographies may be as efficient, given the effective spatial smoothing when averaging across subjects and/or conditions.

Significance: Conservative recommendations for restricting surface Laplacians to high-density recordings may not be appropriate for all ERP research applications, and should be re-evaluated considering objective, costs and benefits.

© 2005 International Federation of Clinical Neurophysiology. Published by Elsevier Ireland Ltd. All rights reserved.

Keywords: Event-related potential (ERP); Dense electrode array (DEA); Current source density (CSD); Low-density surface Laplacian; Principal components analysis (PCA)

1. Introduction

Current source density (CSD) transformation of scalp surface potentials is commonly used as a reference-free method to sharpen ERP topographies in a physiologically-meaningful fashion (e.g. Kayser and Tenke, 2006; Nunez and Westdorp, 1994). CSD or surface Laplacian and other

* Corresponding author. Address: Department of Biopsychology, New York State Psychiatric Institute, Unit 50, 1051 Riverside Drive, New York, NY 10032, USA. Tel.: +1 212 543 5169; fax: +1 212 543 6540.
E-mail address: kayserj@pi.cpmc.columbia.edu (J. Kayser).

deblurring techniques frequently combine high-resolution EEG (64 or more channels) with realistic head models obtained by structural magnetic resonance imaging (e.g. Babiloni et al., 1996, 2000, 2001; Gevins, 1996, 1998; Gevins et al., 1999). In an influential report based on synthetic (i.e. noise-free) and real, single-subject 64-channel ERP data, Junghöfer et al. (1997) have argued that more than 100 recording sites are needed to guarantee reasonable accuracy of surface Laplacian estimates, and concluded 'that nothing meaningful can be inferred about unknown sources' when using a low-density 10–20 system EEG montage. Srinivasan et al. (1998), also using simulated data and 19, 32, 64, or 129 sites of an individual ERP recording to estimate spatial aliasing, similarly concluded that a sufficient density of sensors (i.e. a minimum of 128) is required for adequate spatial sampling of the electrical field at scalp. This conclusion is frequently reiterated, and with it the notion that high-density recordings are a prerequisite for using CSD methodology.[1]

Low-resolution CSDs are sometimes preferable to overresolved CSDs, particularly when the differentiation of sink and source activity is entirely adequate (e.g. Tenke et al., 1993). This assertion rests on the fact that the measured voltage (potential difference) is a volume integral, and is thereby effectively reinforced and stabilized over distance. An overresolved estimate (i.e. when the generator spans a number of electrodes) may be subject to greater measurement and computational noise relative to estimates of the local field potential gradient, from which the CSD is computed. Recent simulation studies have also verified that the advantage of dense electrode recordings for CSD methodology is compromised with increased noise levels (Babiloni et al., 2004; Ryynänen et al., 2004). Moreover, high-density CSD is disproportionately affected by the imprecision in electrode placement, as well as by inter-electrode variability at the electrode-scalp interface (Greischar et al., 2004; Tenke and Kayser, 2001). Sufficient electrode connectivity and accurate (i.e. reliable) scalp placements are affected by a number of variables, including individual differences (e.g. hair texture or scalp dryness) and acquisition hardware (e.g. sensor properties), all of which impact on the signal-to-noise ratio.

In contrast to field potentials, which may be directly measured, CSD waveforms and topographies must always

be estimated, regardless of the simplicity or complexity of model that is used to compute them. The issue, then, is not whether low-density CSDs are perfectly accurate representations of the true Laplacian, but rather whether low-resolution CSDs are helpful for summarizing and interpreting surface potential topographies. In this regard, Babiloni and colleagues have shown the usefulness of low-resolution CSD methodology for clinical settings, in which dense electrode array EEGs may be difficult to record. For example, a 9-channel surface Laplacian used for a brain computer interface (BCI) device provided a reasonable approximation of a full-resolution surface Laplacian (Babiloni et al., 2001). Furthermore, reasonable estimates of both surface Laplacian and low-resolution brain electromagnetic tomography (LORETA; Pascual-Marqui et al., 1994) were obtained from a standard 10–20 system montage consisting of only 19 channels for group data of Alzheimer Disease patients and healthy adults (Cincotti et al., 2004). Likewise, using a subset of 19 electrodes combined with independent component analysis (ICA; Makeig et al., 2000) for estimating event-related synchronization of motor-related beta activity on an individual basis was equally effective as a realistic high-resolution (128-channel) surface Laplacian combined with individual MRI data (Foffani et al., 2004).

While individual CSD topographies may be highly specific and unique, such specificity is largely lost with the analysis of group data. However, a loss of individual specificity is an intentional characteristic for areas of basic research in which the focus is on the discovery of general principles and rules. As pointed out by Junghöfer et al. (1997), averaging over subjects results in spatial low-pass filtering, yielding a loss of spatial resolution when compared to individual averages, but also reducing the error of spatial undersampling. This principle is directly comparable to the temporal low-pass filter resulting from group averages, which can effectively compensate for temporally under-sampled data or an insufficient analog/digital data acquisition and conversion, given the considerable variation in peak latency and amplitude of sequential ERP components across individuals. Despite the uniqueness of individual ERP averages, grand mean ERP waveforms are widely accepted as summaries as long as topographic or latency jitter is acceptable for all comparisons of interests (i.e. groups and/or conditions). Notably, the (temporal) information provided by typical group ERPs recorded at 100 samples/s is not improved by increasing data acquisition to 1000 samples/s, because the highest frequency contribution to the group signal (i.e. less than 10 Hz for P1–N1 amplitude as the steepest deflection) was sufficiently sampled at the lower rate. By analogy, one would expect that the same principles apply to the spatial domain when analyzing and interpreting group data.

To the best of our knowledge, the effects of using more than 100 channels vs. using only a limited 10–20-system montage on the spatial pattern of cognitive ERP activity for

---

[1] During the initial review of our parallel report (Kayser and Tenke, 2006), one reviewer raised the important concern that the number of electrodes used was much too small to reliably estimate CSD, which requires an inter-electrode spacing of less than one inch, or more than 100 channels for complete scalp coverage (e.g. Junghöfer et al., 1997). Arguing that an inadequate spatial sampling of a 31-channel montage will result in artifactual sources and sinks, the reviewer maintained that P3, which is generally assumed to originate from deep and/or distributed sources, should be greatly attenuated in CSD maps. This additional report directly addresses the electrode density problem, which is not only critical for the results and conclusions of that study, but for any other study using low-density CSD estimates.

the analysis of group data have not been reported. Using an existing dense electrode array EEG data set previously recorded from 17 healthy adults during tonal and phonetic oddball tasks (Kayser et al., 2000), and applying unrestricted, temporal principal components analysis (PCA) with Varimax rotation of the covariance loadings (Kayser and Tenke, 2003) as an exhaustive and elaborate approach to summarize high- or low-resolution CSD activity derived from these data, the present study sought to fill this gap by systematically comparing and contrasting high- and low-resolution CSD estimates and their PCA solutions.

2. Methods

2.1. Participants

Out of the original sample of 66 right-handed, healthy adults (see Kayser and Tenke, 2006, for screening details), 24 participants were also tested in a second ERP recording session using a 129-channel geodesic sensor net system (Electrical Geodesics, Inc.). The study had been approved by the institutional review board, and these volunteers, who had given written consent, were again paid $15/h for their participation in this second session, which took place 2–7 days after the first ERP recording session using a 31-channel ElectroCap system (NeuroScan, Inc.). Data from 17 participants (11 men; age range 21–41 years, median = 24, mean = 26.5, SD = 6.3; Edinburgh Handedness Inventory (Oldfield, 1971) laterality quotient = 88.0, SD = 25.6), who provided sufficient artifact-free trials per condition during the 129-channel ERP session, were used in the present CSD analysis.

2.2. Stimuli and procedure

The study design and the procedure of the second 129-channel ERP recording session were essentially identical to the first 31-channel ERP session, using tonal (complex tones) and phonetic (consonant-vowel syllables) oddball tasks with three response modes (left press, right press, silent count) in a complete within-subjects design. Rationale, stimuli, and experimental procedure, which were directly derived from previous studies (Kayser et al., 1998, 2001), are described in detail in our parallel report (Kayser and Tenke, 2006), and, as these aspects are not crucial for the present objective, will for sake of brevity not repeated here. Condition order (i.e. the block sequence constituting task and response mode) was counterbalanced across participants with a latin square. Notwithstanding the ample hard- and soft-ware differences between the two EEG systems, which originate from their different computer platforms (Macintosh vs. IBM-PC), every possible effort was made to keep the experimental features (i.e. stimulus delivery and procedure) as constant as possible across systems. While surface potential results of this ERP study

have previously been presented and discussed in the context of a conventional low- vs. high-density EEG system comparison (Kayser et al., 2000, 2003)[2], the collected dense electrode array (DEA) data perfectly suited the current purpose of evaluating the feasibility of using low-density CSD estimates.

2.3. Data acquisition and recording procedures

Scalp EEG was recorded using a geodesic sensor net (GSN; Tucker, 1993) with a 129-channel, evenly-spaced electrode montage referenced to vertex with a Fpz ground and impedances maintained at 50 kΩ or less using high-impedance amplifiers (200 MΩ; Electrical Geodesics, 1998). In deviation from the standard 129-channel GSN recording montage (for sensor layout and approximate 10–20-system locations, see Fig. 5 in Srinivasan et al., 1998), sensor 17 (nasion) was attached to nose tip to allow offline re-referencing for better comparison with the previously recorded 31-channel ElectroCap data. Continuous EEG data were hardware filtered using a 0.1 Hz high pass (−6 dB/octave), A/D converted (12-bit resolution) at 200 samples/s using an 80 Hz anti-aliasing filter (Electrical Geodesics, 1998), and stored on a Macintosh hard disk using NetStation 1.0 acquisition software (Electrical Geodesics, 1997). Stimulus trigger codes, responses and response latencies were recorded online along with the EEG data for later analyses. Before offline processing, continuous GSN data and stimulus and response codes were converted to raw integer (data) and ASCII (stimulus events) files, ported to a PC platform, and then converted to NeuroScan format. External calibrations (400 µV 20 Hz sine wave, 100 µV step response), which were performed on both EEG systems before data collection, verified nearly identical recording characteristics (e.g. same signal amplitude and offset reduction slope). Horizontal and vertical electrooculograms (EOGs) were calculated offline from facial locations of the dense electrode array. Recording epochs of 1280 ms (including a 200 ms prestimulus baseline) were extracted off-line, tagged for A/D saturation, re-referenced to nose, and low pass filtered at 20 Hz (−24 dB/octave).

2.4. ERP artifact processing and averaging

Blink activity was effectively corrected using a linear regression algorithm applied to the epoched data (Semlitsch et al., 1986). Epochs contaminated by amplifier block or drift, residual blinks, lateral eye movements, muscle activity or movement-related artifacts were tagged by means of an automatic detection criterion of 100 µV signal range (difference between minimum and maximum) on any

---

[2] The symposium presentation of this paper and related animations are available at URL http://psychophysiology.cpmc.columbia.edu/DEA2000.html.

channel. Epochs were also screened for electrolyte bridges (Tenke and Kayser, 2001). To retain a sufficient number of artifact-free trials per condition, and to avoid the ill-effects of excluding individual sites containing artifacts from single epochs (i.e. possibly resulting in a different number of trials per electrode for any given ERP), artifactual data were replaced by spherical spline interpolation (Perrin et al., 1989, 1990) from artifact-free channels if feasible (i.e. artifacts were not restricted to a single region, and replacement was warranted by a sufficient number of channels with clean EEG). Artifact detection and electrode replacement was verified by visual inspection.

For each participant, average ERP waveforms were separately computed from artifact-free trials (correct responses only for button press) for each of the 12 experimental conditions stemming from the combination of task (tonal, phonetic), response mode (left press, right press, silent count), and oddball stimulus (target, frequent). Visual inspections of the individual ERP waveforms prompted the decision to use a minimum criterion of 14 artifact-free trials per condition, warranting that the signal-to-noise ratio was satisfactory for each participant and each condition. This resulted in the exclusion of 7 out of the 24 tested participants. The mean number of trials used to compute these ERP averages from the remaining 17 participants ranged across task and response mode from 23.8 (SD = 4.6) to 26.7 (SD = 3.6) for targets, and from 94.4 (SD = 23.7) to 103.9 (SD = 14.5) for nontargets. ERP waveforms were digitally low-pass filtered at 12.5 Hz (−24 dB/octave), and finally baseline-corrected using the 100 ms preceding stimulus onset.

2.5. Generation of low-density (31-channel) ERP waveforms

A surface potential ERP data set for a conventional low-resolution, 31-channel EEG montage consisting of four midline (Fz, Cz, Pz, Oz) and 13 lateral pairs of tin electrodes (FP1/2, F3/4, F7/8, FC5/6, FT9/10, C3/4, T7/8, CP5/6, TP9/10, P3/4, P7/8, P9/10, O1/2) with a nose tip reference was created from the original 129-channel ERPs using a spherical spline algorithm (Perrin et al., 1989, 1990). The 31-channel EEG montage was identical to our 10–20-system ElectroCap montage used previously, with spherical coordinates specified in our parallel report (cf. Table A1 in Appendix (Supplementary data, doi:10.1016/j.clinph.2005. 08.034) of Kayser and Tenke, 2006). Using the same notation, spherical coordinates of the 129-channel geodesic sensor net as specified by the manufacturer (Electrical Geodesics, Inc.) are given in the Appendix (Supplementary data, doi:10.1016/j.clinph.2005.08.033) of the present report. Evidently due to the evenly-spaced geodesic layout, all 10–20 system locations have no *direct* 129-channel sensor equivalents (vertex and nose being the only exceptions); approximate locations are indicated by Srinivasan et al. (1998). For this reason, low-resolution ERPs exactly

matching our 31-channel EEG montage were interpolated with a spherical spline algorithm (Perrin et al., 1989, 1990) using these 31- and 129-channel spherical coordinates.

2.6. Current source density

The surface Laplacian based on spherical spline functions is considered an excellent interim approach for many research and clinical EEG/ERP applications for which more accurate head models are not practical (Nunez and Westdorp, 1994). All averaged ERP waveforms of both high- (original 129-channel) and low- (interpolated 31-channel) resolution data were transformed into current source density estimates using the spherical spline surface Laplacian algorithm suggested by Perrin et al. (1989, 1990; see appendix of Kayser and Tenke, 2006) with established computation parameters (50 iterations; $m = 4$; $\lambda = 10^{-5}$). CSD estimates were expressed as the negative surface Laplacian of the ERP at each electrode based on a unit sphere (radius $r = 1.0$), and ultimately scaled to Laplacian units ($\mu V/cm^2$) based on a more realistic head radius of 10 cm.

2.7. Data reduction and analysis

To compare and determine common sources of variance in the high- and low-resolution CSD data, the averaged, reference-free CSD waveforms were submitted to temporal principal components analysis (PCA) derived from the covariance matrix, followed by Varimax rotation of the covariance loadings with Kaiser's normalization (Kayser and Tenke, 2003; see also Kayser and Tenke, 2006). Using MatLab code (appendix of Kayser and Tenke, 2003) that emulates the PCA-Varimax algorithms used by BMDP statistical software (program 4M; Dixon, 1992), temporal PCAs were computed for the two CSD data sets (high/low-resolution) using 220 sample points (−100 to 995 ms) as variables (columns), and 26316 (high) or 6324 (low) observations (rows) resulting from the combination of participants (17), task (2), response mode (3), oddball condition (2), and electrode sites (129 or 31). The number of orthogonal factors extracted and retained for Varimax rotation was not restricted by any arbitrary criterion (e.g. Scree test) to maximize the stability and interpretability of meaningful components (Kayser and Tenke, 2003).

As the focus of the present report is to evaluate the comparability of high- and low-resolution CSDs, Pearson's correlations between the grand mean CSD waveforms for tonal and phonetic targets stemming from the high- and low-resolution data sets were computed at each of the 31-channel scalp sites using 220 sample points (−100 to 995 ms) as observations. To again compensate for the lack of directly corresponding surface locations, CSD estimates corresponding exactly to the 31-channel locations were interpolated from the 129-channel CSD data using spherical splines (Perrin et al., 1989, 1990) with the specified 31- and 129-channel coordinates. To evaluate whether low-density

estimates can be used to infer CSD activity at scalp locations not included in the recording montage, additional Pearson's correlations were computed for the 129-channel locations using spherical spline interpolations for the 31-channel CSD data.

Pearson's correlations were also computed between the loadings of high-variance CSD factors stemming from the PCA solutions for the high- and low-resolution data sets (i.e. for the first 10 extracted factors of each solution, each factor explaining at least 0.8% of the total variance).

To evaluate the similarities of factor score topographies derived from high- or low-resolution CSD estimates, Pearson's correlations were computed between the factor scores of corresponding CSD factors for each observed topography, using either 31 or 129 channels as observations, for 17 participants $\times$ 3 response modes (target stimuli only), resulting in 51 correlations per factor and task. Means and standard deviations were then computed from Fisher-Z transformed correlations, and back-transformed to correlation values (mean $\pm$ SD). In addition, Pearson's correlations were computed for the group factor score topographies ($N = 17$). Again, to achieve maximum comparability, high-resolution factor scores used in these correlation analyses were interpolated for corresponding 31-channel locations from the 129-channel factor scores using spherical splines (Perrin et al., 1989, 1990), and, vice versa, for corresponding 129-channel locations from the 31-channel factor scores.

Finally, comparability for statistical effects resulting from analyses of variance (ANOVA) usually performed on the scores for factors of interest was evaluated by repeating the statistical analyses performed in our accompanying report using the same paradigm (Kayser and Tenke, 2006). PCA factor scores for target stimuli stemming from the high (interpolated to 31-channel sites) or low-density PCA solutions were used in repeated measures analysis of variance (ANOVA), with *task* (tonal, phonetic) and *response mode* (left press, right press, silent count) as within-subjects factors, and tailored to the distinct topographic features of each factor by using for each factor a representative subset of recording sites from the 31-channel montage (cf. Kayser and Tenke, 2006). These subsets, which are specified below with the statistical results for each factor, consisted of either midline or lateral, homologous recording sites over both hemispheres, thus adding either *site*, or *site* and *hemisphere* as within-subjects factors to the design. Greenhouse-Geisser epsilon (ε) correction was used to compensate for violations of sphericity when appropriate (e.g. Keselman, 1998).

Behavioral data were analyzed for the sole purpose of verifying similar performance in the 129-channel and 31-channel ERP recording sessions, using separate analyses for button press responses (response latency and percentages of correct responses) and silent counting (estimates of correct responses) as detailed in our parallel report (Kayser and Tenke, 2006).

3. Results

3.1. Behavioral data

Mean response latency for correct button press responses was faster for tones ($M = 435.6$ ms, SD $= 92.2$) compared with syllables ($M = 476.0$ ms, SD $= 107.9$; task main effect, $F_{[1,16]} = 7.27$, $P = .02$). The mean hit rate exceeded 99% in all press conditions (tonal $= 99.5\%$, SD $= 1.6$; phonetic $= 99.1\%$, $SD = 1.6$), with no significant ANOVA effects. A comparable mean hit rate was observed for silent count, revealing marginally significant differences between tonal ($M = 98.3\%$, SD $= 3.3$) and phonetic stimuli ($M = 96.0\%$, SD $= 4.6$; task main effect, $F_{[1,16]} = 3.69$, $P = .07$). These findings indicate a high accuracy in all response conditions, and are highly comparable to those reported for the larger sample ($N = 66$) studied using a conventional 31-channel EEG system (Kayser and Tenke, 2006). They are also in close agreement with our previous behavioral findings using this paradigm (Kayser et al., 1998, 2001).

3.2. Average high- and low-density ERP and CSD waveforms

Grand average ERP waveforms of the original 129-channel and interpolated 31-channel surface potentials were in close correspondence to our previous findings using a nose reference (Kayser and Tenke, 2006; Kayser et al., 1998, 2001). Prominent target ERP components were identified as N1 (peak latency 105 and 115 ms for tonal and phonetic tasks, respectively), N2 (between 200 and 230 ms), and P3 (between 350 and 365 ms). These ERPs showed such a remarkable similarity to those presented in our parallel report (Fig. 2 in Kayser and Tenke, 2006) that another figure in this report seemed unwarranted. Instead, the reference-free CSD transformations of these high- and low-resolution ERP waveforms are given in Fig. 1.[3]

High- and low-resolution CSD waveforms were highly similar at corresponding sites, revealing distinctive CSD components: a lateral temporoparietal source corresponding to a central sink (approximate peak latency 100 ms; e.g. see sites 57/101 vs. TP9/10 and 129 vs. Cz); a lateral temporal sink for tones (155 ms; 46/109 vs. T7/8) but not for syllables; a mid-parietal source for targets, corresponding to an anterior sink (between 300 and 400 ms; 62 vs. Pz, 17 vs. Nose); and a late mid-frontal sink for targets (between 440

---

[3] Animated topographies of the grand mean ERP (not shown) and CSD waveforms (shown in Fig. 1) can be obtained at URL http://psychophysiology.cpmc.columbia.edu/cn2005csd.html.
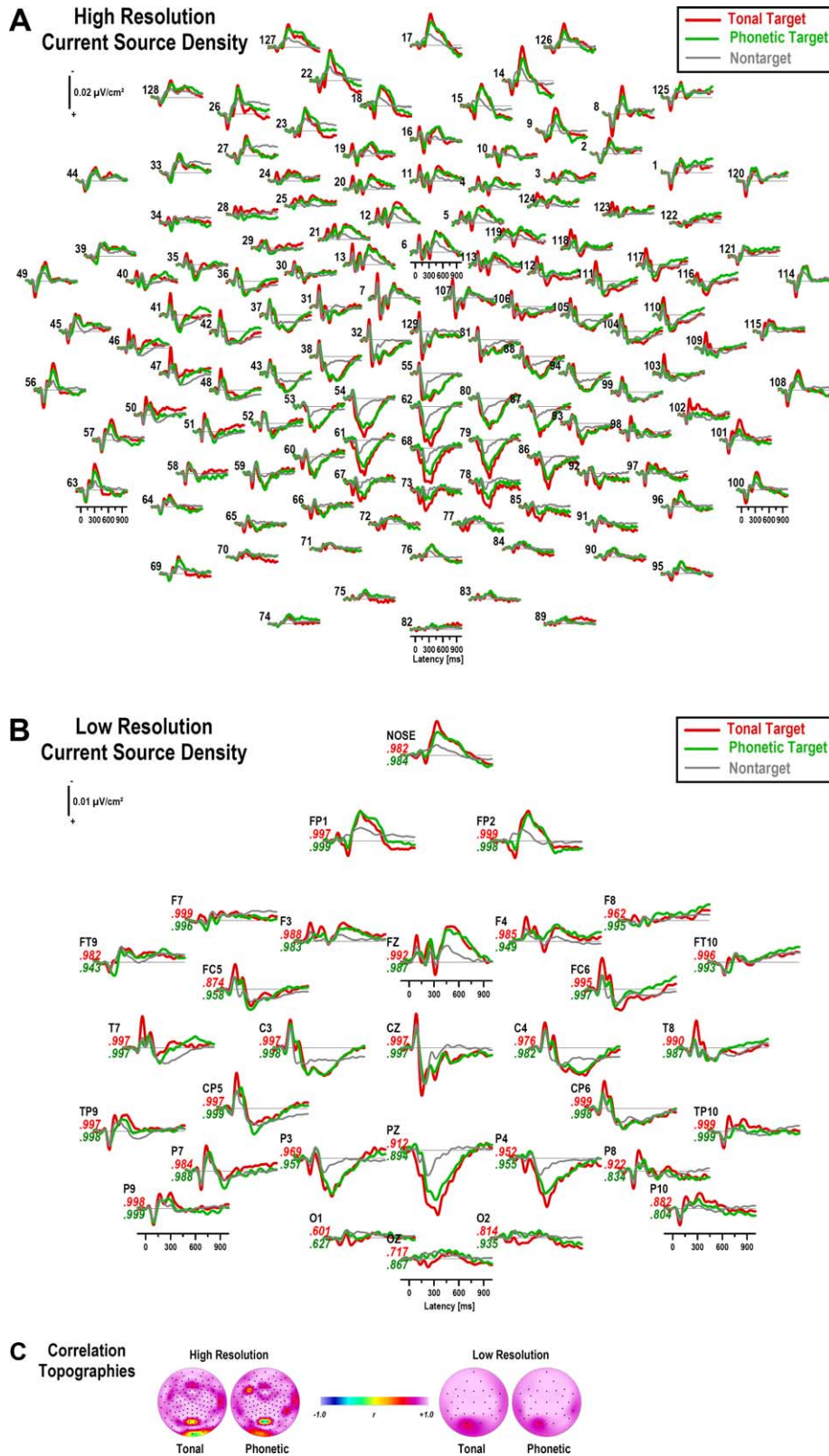
Fig. 1. Reference-free current source density (CSD) waveforms (spherical spline Laplacians; Perrin et al., 1989, 1990) for 17 healthy adults for tonal and phonetic targets (averaged across response mode) and nontargets (averaged across task and response mode). (A) High-resolution CSD estimates were derived from the original surface potentials recorded from 129 scalp locations. (B) Low-resolution CSD estimates were derived from 31 standard (10–20 system) recording sites, for which event-related potentials (ERPs) had been interpolated from the original 129-channel ERPs using a spherical spline algorithm (Perrin et al., 1989, 1990). Pearson's correlations between low- and high-resolution target CSD waveforms at corresponding surface locations are indicated in italics (red: tonal; green: phonetic) below the 10–20 system electrode labels. Note the remarkable similarity between high- and low-resolution CSDs, particularly at

and 690 ms; 5/6/12 vs. Fz). These similarities were resoundingly evidenced by very large Pearson's correlations between corresponding high- and low-resolution CSD waveforms (i.e. for targets of each task), which generally exceeded a value of .9. (cf. green and red italics in Fig. 1B). The only exceptions were sites at the edge of the 31-channel EEG montage that also showed little CSD activity (i.e. where the signal was low; e.g. O1).

The respective correlations at corresponding high-resolution, 129-channel locations (i.e. using the interpolated 129-channel montage from the 31-channel data) are summarized by the topographies shown in the left panel of Fig. 1C (for comparison, correlation topographies of low-resolution, 31-channel locations are shown in the right panel of Fig. 1C). Surprisingly, these CSD waveform correlations were equally high at most sites (i.e. 83 tonal and 84 phonetic target correlations equaled or exceeded $r=.9$, and 109 correlations of each task equaled or exceeded $r=.8$). Although low and even inverse correlations were observed at several occipital sites, and at one left medial-frontal site in the phonetic task, the overall similarity at these interpolated sites is quite remarkable.

3.3. Component waveforms of high- and low-density PCA solutions

A total of 53 factors were sufficient to completely explain the variance in each the two CSD data sets. Fig. 2 compares the time courses of the factor loadings for seven CSD factors of each data set that closely matched those extracted for the larger sample ($N=66$) with conventional 31-channel ERPs (Fig. 4 in Kayser and Tenke, 2006). Factors 1–6 and 9 extracted from the high-resolution CSDs together accounted for 88.9% of the overall CSD variance after Varimax rotation, and factors 1–7 extracted from the low-resolution CSDs accounted for 88.2% total variance. CSD factors were labeled using the peak latency of the factor loadings.

It is immediately apparent from Fig. 2 that both PCA solutions produced corresponding factors with highly comparable variance contributions across solutions, although extraction sequences were slightly different. Moreover, pairwise correlations of factor loadings for the first 10 factors extracted in each PCA solution (total variance 92.2 and 91.6% for high- and low-density data) indicated for each CSD factor a high correspondence ($.946 \leq r \leq .999$) to precisely one CSD factor extracted from the other data set (high- or low-resolution), but negligible correspondence to the remaining factors ($-.391 \leq r \leq .707$). The highest unique correlations
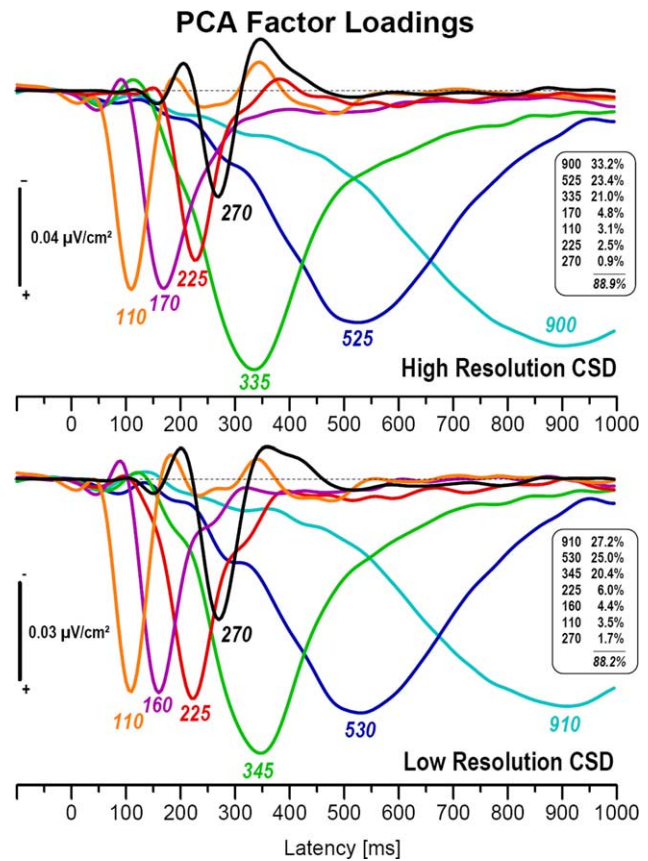
Fig. 2. Time courses of factor loadings for PCA components extracted from high- (top) and low-resolution CSD (current source density; bottom) waveforms. CSD factor labels indicate the peak latency of the factor loadings; for better comparability, corresponding factor loadings of the two solutions were plotted in corresponding colors, and scales were marginally adjusted to approximate loadings' amplitudes. Insets indicate the percentage of explained variance after Varimax rotation for each factor (This figure appears in colour on the web).

($.990 \leq r \leq .999$) were obtained for the first three CSD factors (i.e. between factors 900 and 910, 525 and 530, and 335 and 345) and CSD factors 110, strongly suggesting that these temporal PCA measures are stable and reproducable for high- and low-resolution CSD data sets.

3.4. Component topographies of high- and low-density PCA solutions

The factor score topographies of the PCA solutions derived from high- and low- resolution CSD data sets are depicted in Fig. 3 for target stimuli in both tasks (averaged across response mode). As can be easily seen, high-resolution CSD topographies are in close agreement with

recording sites showing high signal-to-noise ratio (e.g. 129 vs. Cz, 6 vs. Fz, 62 vs. Pz, 46/109 vs. T7/T8). (C) Topographies of Pearson's correlations between high- and low-resolution target CSD waveforms at surface locations corresponding to the high (left maps) or low (right maps) density montage. CSD estimates corresponding exactly to the 129-channel locations were interpolated from the 31-channel CSD data, and vice versa for the low-density montage (31-channels interpolated from 129-channel CSDs). Note that these correlation maps were generated using flexible splines without additional smoothing ($m=2$; $\lambda=0$; cf. Kayser and Tenke, 2006) to facilitate comparisons of high-density correlations to the low-density correlations already indicated in B (For interpretation of the reference to colour in this legend, the reader is referred to the web version of this article).
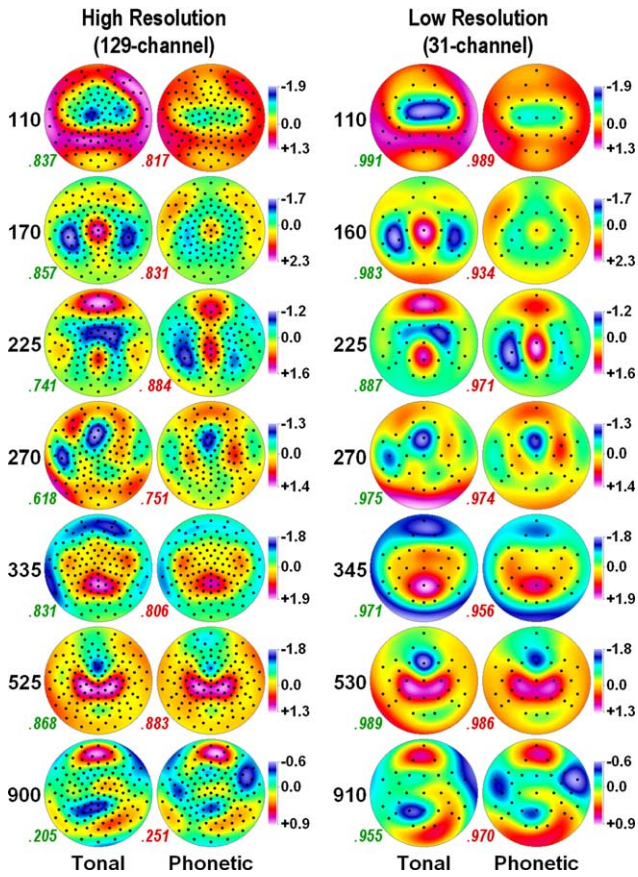
Fig. 3. Mean topographies of factor scores ($N=17$) for PCA components extracted from high- (left) and low- (right) resolution CSD (current source density) waveforms. Topographies are shown for tonal (columns 1 and 3) and phonetic (columns 2 and 4) target stimuli only (averaged across response mode), and ordered from top to bottom according to the peak latency of the factor loadings. Black dots indicate the spherical positions of the 129- and 31-channel EEG montage (nose at top). All topographic maps are 2D-representations of spherical spline surface interpolations (Perrin et al., 1989, 1990; see Appendix of Kayser and Tenke, 2006) derived from the mean factors scores available for each recording site. To improve comparability across solutions, the same scale was applied for each pair of corresponding factors (i.e. for each row). Pearson's correlations between low- and high-resolution CSD factor scores of group topographies (i.e. using either 129 or 31 sites as observations, and interpolating corresponding surface locations from the spatially over- or under-sampled montage) are indicated for tonal and phonetic targets (green and red italics) (For interpretation of the reference to colour in this legend, the reader is referred to the web version of this article).

low-resolution CSD topographies for corresponding factors and conditions; in fact, it is harder to indicate their subtle differences. Moreover, these factor score topographies are almost identical to the low-resolution CSD topographies reported in our parallel report (Fig. 5 in Kayser and Tenke, 2006).

Both the high- and low-resolution factor 110 overlapped the central sink (corresponding to N1 in the surface potentials) and the lateral temporo-parietal source peaking around 100 ms, and showed a corresponding negative amplitude over medial-central sites and a positive amplitude over lateral temporo-parietal sites, which was larger for tones

than syllables (Fig. 3, top row). Although the high-resolution CSD topographies suggested a separation of this central sink over each hemisphere, which is in close correspondence to the low-resolution topographies of this factor for the larger sample (cf. Fig. 5 in Kayser and Tenke, 2006), the low-density CSD topographies of this factor are nevertheless an accurate approximation.

Similarly, the high- and low-resolution factors summarizing a tonal temporal N1 (170 and 160) were both characterized by a prominent lateral temporo-parietal sink for the tonal task, with a corresponding source maximal over vertex (Fig. 3, second row).

Both high- and low-resolution PCA solutions summarized the task- and regional-specific hemispheric asymmetries associated with N2 in a single CSD factor (225), revealing distinct right-lateralized mid-frontal sinks for the tonal task, and left-lateralized temporo-parietal sinks for the phonetic task (Fig. 3, third row).

A prominent medial-parietal source corresponding a classical P3b amplitude for targets, which extended to lateral-temporal sites and also included a fronto-polar sink, was evident in both high- and low-resolution CSD topographies of factors 335 and 345 (Fig. 3, fifth row). Although source contributions were somewhat better resolved for the high-density solution, the low-density CSD topographies of this factor are again highly appropriate approximations.

As found for the low-resolution CSDs using a larger sample and a conventional EEG system (Kayser and Tenke, 2006), both the high- and low-resolution CSD-PCA of the present smaller sample using geodesic sensor net EEG recordings produced a distinct high-variance factor following the peak of P3b (factors 525 and 530). The factors' topography was characterized by a large, focal sink effectively restricted to a narrow, mid-frontal region (sites 5, 6, and 12; site Fz), and two mid-central sources over somatosensory regions (Fig. 3, sixth row), essential replicating the finding for the larger sample.

Finally, even the factors not considered for statistical analysis in our parallel report (Kayser and Tenke, 2006) revealed the same level of similarity between high- and low-density CSD solutions for these group topographies (i.e. factors 270 and 900/910; Fig. 3, fourth and last row).

The similarity between the high- and low-resolution CSD group topographies was also clearly supported by the Pearson's correlations between the factor scores derived from the high- and low-density PCA solutions for corresponding factors using corresponding sites (i.e. for targets of each task). For the low-density, 31-channel group topographies, these correlations were $.887 \leq r \leq .991$ (cf. green and red italics in Fig. 3, right columns). For the high-density, 129-channel group topographies (i.e. interpolating the spatially-undersampled 31-channel CSD data), these correlations were $.205 \leq r \leq .884$ (cf. green and red italics in Fig. 3, left columns); however, the ranges were

Table 1
Pearson's correlations for corresponding CSD factor scores of high and low-density PCA solutions (target stimuli only) using corresponding scalp locations

Factors	Tonal			Phonetic		
	r_{mean}	r_{SD}	$r_{N=17}$	r_{mean}	r_{SD}	$r_{N=17}$
Low-resolution						
110/110	0.980	0.965–0.989	0.991	0.973	0.949–0.986	0.989
170/160	0.944	0.888–0.973	0.983	0.904	0.851–0.939	0.934
225/225	0.884	0.779–0.942	0.887	0.925	0.869–0.957	0.971
270/270	0.954	0.921–0.973	0.975	0.945	0.901–0.970	0.974
335/345	0.957	0.928–0.974	0.971	0.956	0.929–0.973	0.956
525/530	0.968	0.943–0.983	0.989	0.972	0.951–0.984	0.986
900/910	0.960	0.932–0.977	0.955	0.958	0.926–0.977	0.970
High-resolution						
110/110	0.534	0.330–0.690	0.837	0.384	0.155–0.575	0.821
170/160	0.443	0.219–0.622	0.857	0.393	0.147–0.593	0.831
225/225	0.503	0.255–0.689	0.741	0.308	0.099–0.491	0.884
270/270	0.046	−0.170–0.257	0.618	0.132	−0.116–0.365	0.751
335/345	0.501	0.241–0.694	0.831	0.474	0.213–0.671	0.806
525/530	0.398	0.203–0.563	0.868	0.427	0.241–0.582	0.883
900/910	0.170	−0.040–0.364	0.205	0.111	−0.089–0.301	0.251

Note. Correlations were computed for each corresponding CSD topography (31-channel montage: high-resolution factor scores interpolated for corresponding 31-channel locations; 129-channel montage: low-resolution factor scores interpolated for corresponding 129-channel locations; 17 participants × 3 response modes = 51 correlations/factor/task). Means and standard deviations (SD) were computed from Fisher-Z transformed correlations, averaged, and back-transformed (Bortz, 1985); correlations of group topographies ($N = 17$) did not require this transformation.

$.741 \leq r \leq .884$ for the meaningful five factors considered for statistical analyses in our parallel report (Kayser and Tenke, 2006).

The mean correlations (and their standard deviations) of the individual factor score topographies for tonal and phonetic targets are given in Table 1, and compared to the correlations of the group factor score topographies. For the low-resolution, 31-channel topography (interpolated for the 129-channel CSD factor scores), these individual correlations are in close agreement with those for the group topographies (upper panel of Table 1), suggesting high similarity of low-resolution CSD topographies even on an individual (i.e. case) level. For the high-resolution, 129-channel topography (interpolated for the 31-channel CSD factor scores), the individual correlations were substantially lower than those for the group topographies (lower panel of Table 1), ranging between .308 and .533 for the five meaningful CSD factors, suggesting a notably higher variability of individual, high-resolution CSD topographies. Interestingly, the correlations for the two factors not considered for statistical analyses in our companion paper (i.e. factors 270/270 and 900/910; cf. Kayser and Tenke, 2006) were particularly low for the averaged individual topographies ($.046 \leq r \leq .170$), indicating a low validity of these factors and in retrospect vindicating the decision to not consider them.

3.5. Comparability of repeated measures ANOVA test statistics

Statistical analysis was performed on the scores of five pairs of corresponding, physiologically-meaningful PCA factors derived from high (129-channel) or low (31-channel)

density CSD estimates (i.e. high/low: 110/110, 170/160, 225/225, 335/345, 525/530). Eight repeated measures ANOVA were calculated for each PCA solution using: medial-central sites (C3/4) for factors 110/110; either lateral-temporal sites (T7/8) or the mid-central site (Cz) for factors 170/160; five homologous pairs of either fronto-central (F3/4, F7/8, FC5/6, C3/4, FT9/10) or centro-temporo-parietal sites (P7/8, P9/10, CP5/6, T7/8, TP9/10) for factors 225/225; three homologous pairs of medial and lateral centro-parietal sites (P34, CP56, P78) for factors 335/345; and either the mid-frontal site (Fz) or medial-central sites (C3/4) for factors 525/530 (cf. Kayser and Tenke, 2006). The F values of all effects[4] stemming for these parallel analyses are given in Fig. 4. As can be seen, the statistical effects tested in these analyses were highly comparable between high and low-density CSD estimates, that is, significant and insignificant effects (i.e. interactions and main effects having either large or small F values) were identified in close correspondence. Although F values occasionally exceeded the critical significance threshold of $P = .05$ in one data set but not the other, these cases constitute more a problem of statistical convention for null hypothesis testing (i.e. a significance of $P = .04$ is usually not significantly different from a significance of $P = .06$; cf. Greenwald et al., 1996) than qualifying the overall impression of high compatibility of F statistics when using either high- or low-density CSD estimates at previously-identified, low-density recording sites.

---

[4] Because all factor scores for each extracted factor are standardized (mean = 0.0; SD = 1.0), the significance tests for the grand mean (significant difference from zero) for the selected subset of electrodes are meaningful and therefore included.
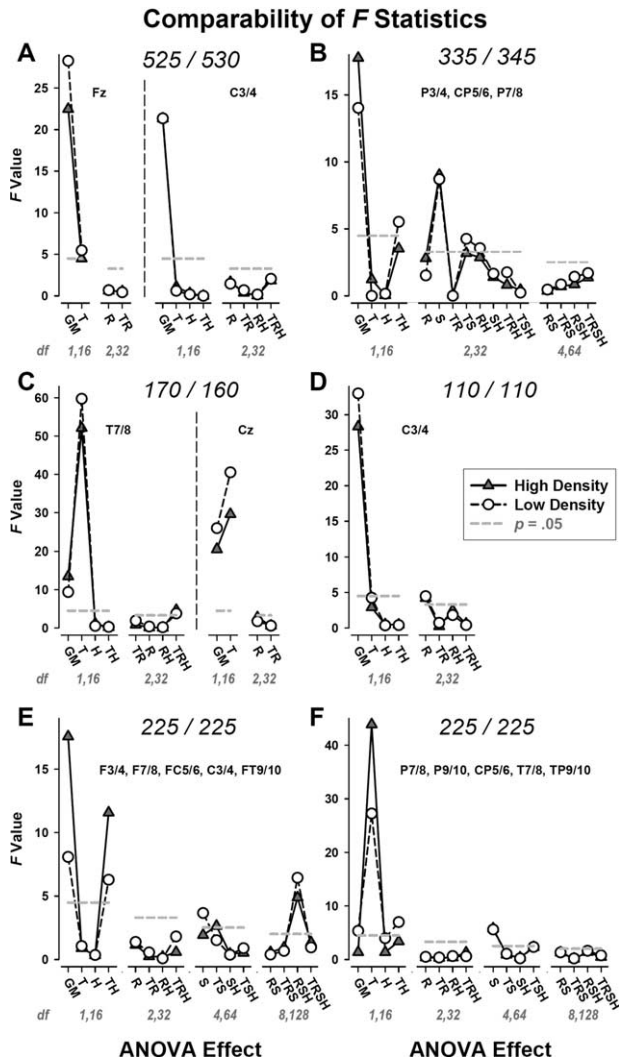
Fig. 4. Comparison of statistical effects (*F* values) of repeated measures analyses of variance (ANOVA) performed on corresponding, physiologically-meaningful PCA factor scores (i.e. 525/530, 335/345, 170/160, 110/110, 225/225) derived from high (129 channels; triangles) and low (31channels; circles) density CSD estimates. The repeated measures ANOVA design consisted of task (tonal, phonetic) and response mode (left press, right press, silent count; target stimuli only), and, if required, hemisphere and site to account for the selected subset of electrodes as indicated (cf. Kayser and Tenke, 2006). The different degrees of freedom (df) are listed below the various main effects and interactions (GM, Grand Mean; T, Task; H, Hemisphere; R, Response Mode; S, Site). The corresponding conventional level of significance (*P* = .05) is indicated for convenience (horizontal dashes), but does not reflect Greenhouse-Geisser epsilon corrections where appropriate.

4. Discussion

Surface Laplacian estimates derived from a standard 31-channel, 10–20 system EEG montage with an established spherical spline interpolation (Perrin et al., 1989, 1990) were found to be surprisingly accurate approximations of CSD estimates derived from a 129-channel, dense electrode array using the same spherical spline interpolation. For a group of 17 healthy adults, grand mean CSD waveforms

and all identified CSD components, using unrestricted temporal PCA as an efficient means to exhaustively summarize data variance (Kayser and Tenke, 2003), as well as their ensuing *F* statistics, were virtually identical for a low-density, 31-channel CSD montage derived from high- and low-density ERP recordings. Reasonable approximations of high-density CSD activity could still be obtained from interpolations of low-density group, but not individual, data. In other words, low-density CSD estimates were not only adequate, but sufficient to fully describe the variance of a typical ERP data set collected during an auditory oddball paradigm, and there was no apparent advantage of using high-density CSD transformations. These results are in close accordance with recent evidence collected in a clinical context, revealing that a sufficient degree of accuracy can be achieved with low-resolution CSD methodology combined with a quasi-realistic (i.e. averaged) head model, almost equivalent to what would have been obtained from high-resolution surface Laplacian estimates combined with individual MRIs (e.g. Babiloni et al., 2001; Concotti et al., 2004; Foffani et al., 2004).

While these findings appear to contradict previous recommendations that an evenly-spaced EEG montage with inter-electrode distances of about 1 in. (i.e. 100 channels or more) is needed to accurately estimate sources and sinks at scalp (e.g. Junghöfer et al., 1997; Srinivasan et al., 1998), this discrepancy can be reconciled if one considers that the rationale for these recommendations relied on simulated and individual data. As observed here, high-density CSD estimates derived from interpolated low-density CSD data were clearly less comparable for individual topographies. By averaging ERPs across many individuals, spatial and temporal noise levels can be reduced, thereby removing group-unspecific ERP contributions and increasing the group-specific signal-to-noise ratio (SNR), analogous to the removal of unsystematic (i.e. not time-locked) background activity when averaging EEG epochs over many trials to improve the subject-specific SNR. The spatial low-pass filter resulting from group averages is a desirable characteristic for a basic research objective that is less concerned with individual variations of neuronal function and anatomy, but is instead focused on brain processes that can be generalized to the population under study. Evidently, such general principles can be efficaciously inferred from low-density CSD estimates of ERP data (Kayser and Tenke, 2006), or when used to obtain reference-free EEG spectra (Tenke and Kayser, 2005).

This systematic comparison between high- and low-density CSDs shows that the use of a low-density recording montage has no impact on the applicability of the new methods and findings reported in our parallel study (Kayser and Tenke, 2006), which allowed us to disentangle distinct neuronal generator patterns of response-related (i.e. left or right button press vs. silent count) and task-related (i.e. detection of tonal or phonetic targets) processes. Although it is not quite clear to what extent the current findings also

apply to other ERP paradigms, it is not very likely that one would arrive at a different conclusion regarding the comparability and adequacy of low-density CSD estimates when employing a different ERP task, given that this paradigm involves rather subtle and highly-specific topographic effects (e.g. regional task × hemisphere interactions; cf. Kayser and Tenke, 2006). However, it remains to be seen whether a low-density surface Laplacian is sufficient for the analysis of group ERP data in all cases.

It also remains to be decided whether a spatial or spatiotemporal PCA (Spencer et al., 1999, 2001), when applied to CSD waveforms, or other multivariate approaches exploiting spatiotemporal ERP characteristics (e.g. Lobaugh, West, and McIntosh, 2001; Makeig et al., 1997), may result in notable differences between high- and low-density ERP recordings for group data. On a theoretical level, it could be argued that by focusing on spatial variance (although it must be noted that spatial variance also contributes to factor extraction in a temporal PCA; Kayser and Tenke, 2003, 2005), the benefits of a dense electrode array become more important. On the other hand, if the benefits of spatial enhancement are highly variable across individuals, one would expect that spatial PCA or related approaches will also result in largely comparable findings for high- and low-density ERP recordings.

As a final caution, the properties of the Laplacian transformation should be considered. For instance, consistent with our previous studies using a standard 31-channel EEG montage (Kayser and Tenke, 2006; Tenke et al., 1998), we have used spherical spline interpolations with constants $m=4$ and $\lambda=10^{-5}$ for both high- and low-density data sets for comparability reasons, whereas more flexible splines (i.e. $m=3$ or 2; cf. Eq. (2) of Kayser and Tenke, 2006) could be used with dense electrode arrays to allow for a greater proportion of higher spatial frequencies (cf. Junghöfer et al., 1997). After applying a more flexible spline function ($m=3$) to the current 129-channel data set, computational noise levels were considerably higher when compared to the more rigid spline function ($m=4$), especially at the edges of the EEG montage, but the ensuing temporal PCA nevertheless extracted essentially the same set of factors. Moreover, highly similar findings were obtained when a local Hjorth was applied to the present high-density ERP data (Kayser et al., 2000). This convergence of different surface Laplacian models is also in agreement with previous CSD findings using 31-channel (Tenke et al., 1998) or even 21-channel ERP recordings (Tandonnet et al., 2005).

In conclusion, the present study strongly argues against a categorical rejection of low-density CSD estimates as valid means to infer neuronal generator patterns from group data. Rather, previous recommendations that at least 100 or more EEG channels be required before computing surface Laplacians should be re-evaluated on the basis of the given research objective and scenario. The need for a re-evaluation should not be limited to circumstances in which recording EEG with dense electrode arrays are not

feasible (or are undesirable), such as for certain clinical studies (e.g. Babiloni et al., 2001; Concotti et al., 2004; Foffani et al., 2004). Even basic research studies targeting healthy populations would be well-advised to consider the costs and benefits of engaging in high-density EEG recordings, which require a significantly greater amount of time to administer and process, may introduce additional error or noise related to the precision and density of electrode placement (Greischar et al., 2004; Tenke and Kayser, 2001), and may even leave the investigator unprepared to adequately manage the vast quantity of data (cf. Kayser and Tenke, 2005). This direct comparison leaves no doubt that advanced CSD techniques can be appropriately and successfully applied to a conventional 10–20 system EEG recording montage.

Supplementary data

Supplementary data associated with this article can be found at doi:10.1016/j.clinph.2005.08.033

References

Babiloni F, Babiloni C, Carducci F, Fattorini L, Onorati P, Urbano A. Spline Laplacian estimate of EEG potentials over a realistic magnetic resonance-constructed scalp surface model. Electroencephalogr Clin Neurophysiol 1996;98(4):363–73.

Babiloni F, Babiloni C, Locche L, Cincotti F, Rossini PM, Carducci F. High-resolution electro-encephalogram: source estimates of Laplacian-transformed somatosensory-evoked potentials using a realistic subject head model constructed from magnetic resonance images. Med Biol Eng Comput 2000;38(5):512–9.

Babiloni F, Cincotti F, Carducci F, Rossini PM, Babiloni C. Spatial enhancement of EEG data by surface Laplacian estimation: the use of

magnetic resonance imaging-based head models. Clin Neurophysiol 2001;112(5):724–7.

Babiloni F, Babiloni C, Carducci F, Romani GL, Rossini PM, Angelone LM, Cincotti F. Multimodal integration of EEG and MEG data: a simulation study with variable signal-to-noise ratio and number of sensors. Hum Brain Mapp 2004;22(1):52–62.

Bortz J. Lehrbuch der Statistik. Berlin: Springer; 1985.

Cincotti F, Babiloni C, Miniussi C, Carducci F, Moretti D, Salinari S, Pascual-Marqui R, Rossini PM, Babiloni F. EEG deblurring techniques in a clinical context. Methods Inf Med 2004;43(1):114–7.

Dixon WJ, editor. BMDP statistical software manual: to accompany the 7.0 software release. Berkeley, CA: University of California Press; 1992.

Electrical Geodesics, Inc. Net station manual. Eugene, OR: Author; 1997.

Electrical Geodesics, Inc. Electrical geodesics. Eugene, OR: Author; 1998.

Foffani G, Bianchi AM, Cincotti F, Babiloni C, Carducci F, Babiloni F, Rossini PM, Cerutti S. Independent component analysis compared to Laplacian filtering as 'deblurring' techniques for event related desynchronization/synchronization. Methods Inf Med 2004;43(1):74–8.

Gevins A. High resolution evoked potentials of cognition. Brain Topogr 1996;8(3):189–99.

Gevins A. The future of electroencephalography in assessing neurocognitive functioning. Electroencephalogr Clin Neurophysiol 1998;106(2):165–72.

Gevins A, Smith ME, McEvoy LK, Leong H, Le J. Electroencephalographic imaging of higher brain function. Philos Trans R Soc Lond B Biol Sci 1999;354(1387):1125–33.

Greenwald AG, Gonzalez R, Harris RJ, Guthrie D. Effect sizes and *p* values: what should be reported and what should be replicated? Psychophysiology 1996;33(2):175–83.

Greischar LL, Burghy CA, van Reekum CM, Jackson DC, Pizzagalli DA, Mueller C, Davidson RJ. Effects of electrode density and electrolyte spreading in dense array electroencephalographic recording. Clin Neurophysiol 2004;115(3):710–20.

Junghöfer M, Elbert T, Leiderer P, Berg P, Rockstroh B. Mapping EEG-potentials on the surface of the brain: a strategy for uncovering cortical sources. Brain Topogr 1997;9(3):203–17.

Kayser J, Tenke CE. Optimizing PCA methodology for ERP component identification and measurement: theoretical rationale and empirical evaluation. Clin Neurophysiol 2003;114(12):2307–25.

Kayser J, Tenke CE. Trusting in or breaking with convention: towards a renaissance of principal components analysis in electrophysiology. Clin Neurophysiol 2005;116(8):1747–53.

Kayser J, Tenke CE. Principal components analysis of Laplacian waveforms as a generic method for identifying ERP generator patterns: I. Evaluation with auditory oddball tasks. Clin Neurophysiol 2006;117(2):348–68.

Kayser J, Tenke CE, Bruder GE. Dissociation of brain ERP topographies for tonal and phonetic oddball tasks. Psychophysiology 1998;35(5):576–90.

Kayser J, Tenke CE, Bhattacharya N, Stuart BK, Hudson J, Bruder GE. A direct comparison of geodesic sensor net (128-channel) and conventional (30-channel) ERPs in tonal and phonetic oddball tasks. Psychophysiology 2000;37:S17 http://psychophysiology.cpmc.columbia.edu/DEA2000.html.

Kayser J, Bruder GE, Tenke CE, Stuart BK, Amador XF, Gorman JM. Event-related brain potentials (ERPs) in schizophrenia for tonal and phonetic oddball tasks. Biol Psychiatry 2001;49(10):832–47.

Kayser J, Tenke CE, Bruder GE. Evaluating the quality of ERP measures across recording systems: a commentary on Debener et al. (2002). Int J Psychophysiol 2003;48(3):315.

Keselman HJ. Testing treatment effects in repeated measures designs: an update for psychophysiological researchers. Psychophysiology 1998;35(4):470–8.

Lobaugh NJ, West R, McIntosh AR. Spatiotemporal analysis of experimental differences in event-related potential data with partial least squares. Psychophysiology 2001;38(3):517–30.

Makeig S, Jung TP, Bell AJ, Ghahremani D, Sejnowski TJ. Blind separation of auditory event-related brain responses into independent components. Proc Natl Acad Sci USA 1997;94(20):10979–84.

Makeig S, Enghoff S, Jung TP, Sejnowski TJ. A natural basis for efficient brain-actuated control. IEEE Trans Rehabil Eng 2000;8(2):208–11.

Nunez PL, Westdorp AF. The surface Laplacian, high resolution EEG and controversies. Brain Topogr 1994;6(3):221–6.

Oldfield RC. The assessment and analysis of handedness: the Edinburgh inventory. Neuropsychologia 1971;9(1):97–113.

Oostenveld R, Praamstra P. The five percent electrode system for high-resolution EEG and ERP measurements. Clin Neurophysiol 2001;112(4):713–9.

Pascual-Marqui RD, Michel CM, Lehmann D. Low resolution electromagnetic tomography: a new method for localizing electrical activity in the brain. Int J Psychophysiol 1994;18(1):49–65.

Perrin F, Pernier J, Bertrand O, Echallier JF. Spherical splines for scalp potential and current density mapping [Corrigenda EEG 02274, Clin. Neurophysiol, 1990, 76, 565]. Electroencephalogr Clin Neurophysiol 1989;72(2):184–7.

Perrin F, Pernier J, Bertrand O, Echallier JF. Corrigenda EEG 02274. Electroencephalogr Clin Neurophysiol 1990;76:565.

Ryynänen OR, Hyttinen JA, Laarne PH, Malmivuo JA. Effect of electrode density and measurement noise on the spatial resolution of cortical potential distribution. IEEE Trans Biomed Eng 2004;51(9):1547–54.

Semlitsch HV, Anderer P, Schuster P, Presslich O. A solution for reliable and valid reduction of ocular artifacts, applied to the P300 ERP. Psychophysiology 1986;23(6):695–703.

Spencer KM, Dien J, Donchin E. A componential analysis of the ERP elicited by novel events using a dense electrode array. Psychophysiology 1999;36(3):409–14.

Spencer KM, Dien J, Donchin E. Spatiotemporal analysis of the late ERP responses to deviant stimuli. Psychophysiology 2001;38(2):343–58.

Srinivasan R, Tucker DM, Murias M. Estimating the spatial Nyquist of the human EEG. Behav Res Methods Instrum Comput 1998;30(1):8–19.

Tandonnet C, Burle B, Hasbroucq T, Vidal F. Spatial enhancement of EEG traces by surface Laplacian estimation: comparison between local and global methods. Clin Neurophysiol 2005;116(1):18–24.

Tenke CE, Kayser J. A convenient method for detecting electrolyte bridges in multichannel electroencephalogram and event-related potential recordings. Clin Neurophysiol 2001;112(3):545–50.

Tenke CE, Kayser J. Reference-free quantification of EEG spectra: Combining current source density (CSD) and frequency principal componenets analysis (fPCA). Clin Neurophysiol 2005;116(12):2826–46.

Tenke CE, Schroeder CE, Arezzo JC, Vaughan Jr HG. Interpretation of high-resolution current source density profiles: a simulation of sublaminar contributions to the visual evoked potential. Exp Brain Res 1993;94(2):183–92.

Tenke CE, Kayser J, Fong R, Leite P, Towey JP, Bruder GE. Response- and stimulus-related ERP asymmetries in a tonal oddball task: a Laplacian analysis. Brain Topogr 1998;10(3):201–10.

Tucker DM. Spatial sampling of head electrical fields: the geodesic sensor net. Electroencephalogr Clin Neurophysiol 1993;87:154–63.